A tailored extracellular matrix (ECM) - Mimetic coating for cardiovascular stents by stepwise assembly of hyaluronic acid and recombinant human type III collagen

Li Yang [a], Haoshuang Wu [a], Lu Lu [b], Qing He [a], Boting Xi [a], Hongchi Yu [a], Rifang Luo [a,**], Yunbing Wang [a,*], Xingdong Zhang [a]

[a] National Engineering Research Center for Biomaterials, Sichuan University, Chengdu, 610064, China
[b] Key Laboratory of Medical Molecular Virology (MOE/NHC/CAMS), School of Basic Medical Sciences and Shanghai Public Health Clinical Center, Fudan-Jinbo Joint Research Center, Fudan University, Shanghai, 200302, China

ARTICLE INFO

ABSTRACT

Collagen, a central component of the extracellular matrix (ECM), has been widely applied in tissue engineering, among others, for wound healing or bone and nerve regeneration. However, the inherent thrombogenic properties of collagen hinder the application in blood-contacting devices. Herein, a brand-new recombinant human type III collagen (hCOLIII) was explored that does not present binding sites for platelets while retaining the affinity for endothelial cells. The hCOLIII together with hyaluronic acid (HA) were deposited on the substrates via layer-by-layer assembly to form an ECM-mimetic multilayer coating. In vitro platelet adhesion and ex vivo blood circulation tests demonstrated prominent thromboprotective properties for the hCOLIII-based ECM-mimetic coating. In addition, the coating effectively guided the vascular cell fate by supporting the proliferation of endothelial cells and inhibiting the proliferation of smooth muscle cells by differentiating them to a more contractile phenotype. A polylactic acid (PLA) stent coated with hCOLIII-based ECM-mimetic coating was implanted in the abdominal aorta of rabbits to investigate the healing of the neointima. The enhanced endothelialization, suppressed inflammatory response, inhibition of excessive neointimal hyperplasia, and the superior thromboprotection strongly indicated the prospect of the hCOLIII-based ECM-mimetic coating as a tailored blood-contacting material for cardiovascular stents.

1. Introduction

Cardiovascular stent implantation has become the most essential tool for treating coronary heart disease (CVD), the primary killer threatening human life [1,2]. However, stent implantation causes acute vascular vessel damage, followed by the risk of thrombus formation, acute inflammatory response, and excessive hyperplasia [3]. Therefore, ideal stent coatings, whether used alone or combined with drugs, should be multifunctional, promote rapid in-situ endothelialization, inhibit the hyperplasia of smooth muscle cells (SMCs), and prevent the adhesion of inflammatory cells [4–6]. Functional stent coatings to support the rapid proliferation of endothelial cells have been developed via introducing bioactive molecules, like vascular endothelial growth factor (VEGF), short adhesive peptides (including Arg-Glu-Asp-Val (REDV),

Arg-Gly-Asp (RGD)), integrin-associated protein (IAP or CD47), and extracellular matrix (ECM) components (including fibronectin, laminin, and hyaluronic acid) [7–9]. Although the introduction of bioactive molecules exhibited good application prospects in vitro, the non-selectivity in guiding the proliferation of SMCs, and the promotion of thrombus deposition were severe obstacles to the further development of the techniques [10].

Collagen, the dominant component in the ECM, provides the basic structure and mechanical support of most tissues, and is widely applied in tissue engineering, wound healing, bone and nerve regeneration applications [11,12]. Collagen is usually used as a blend with other natural or synthetic polymers. For instance, collagen was mixed among others with keratin, silk protein, chitosan, hyaluronic acid to simulate the basic structure of a specific ECM and the required function is further

---

mimicked by growth factors [13,14]. Though animal-derived collagen, mainly obtained from tendon or skin, is widely employed in tissue engineering, its inherent thrombogenicity (platelets activation) restricts its application in vascular devices, such as vascular stents, artificial heart valves, vascular grafts, circulation catheters (e.g. central venous catheter (CVC), or tubes for extracorporeal membrane oxygenation (ECMO) or dialysis) [15,16].

Can collagen be used as a blood-contacting material? Advanced technologies may open this possibility. Peptide synthesis, genetic engineering, and fermentation engineering are powerful tools for tailoring desired peptides/proteins and realizing industrial production [17–19]. We previously found by tailored design that a protein sequence derived from human type III collagen, containing Gly-Glu-Arg (GER) and Gly-Glu-Lys (GEK) triplets, provides potent cell adhesion activity [20]. The recombinant protein has a stable triple-helix conformation and multiple charged residues. The cell adhesion is mediated by

integrin-binding to the peptides [20,21]. Collagen activates platelets via the receptors GP Ia/IIa ($\alpha_2\beta_1$), GP VI, and GP Ib/IX/V complexes [22, 23]. The I domain of the receptor $\alpha2\beta1$ recognizes and binds collagen at the sequences GFOGER, GLOGER, GROGER, GLOGEN, etc., leading to severe platelet adhesion and activation [24]. These sequences suggest that hydroxyproline (O) in the triple-helix fragment probably is essential platelet adhesion and activation. Thus, engineering a recombinant protein with large amounts of cell adhesive motives, such as GER or GEK, but without hydroxyproline-containing fragments might provide an option for developing a tailored collagen for use in blood-contact. In addition, immunogenicity, poor water solubility, and batch-to-batch variabilities of animal-derived collagen (aCOL) further restrict its wide application, especially in the preparation of collagen-based coatings on biomedical implants [25,26]. The recombinant collagen is also considered to provide better water solubility and low inflammatory response [21].
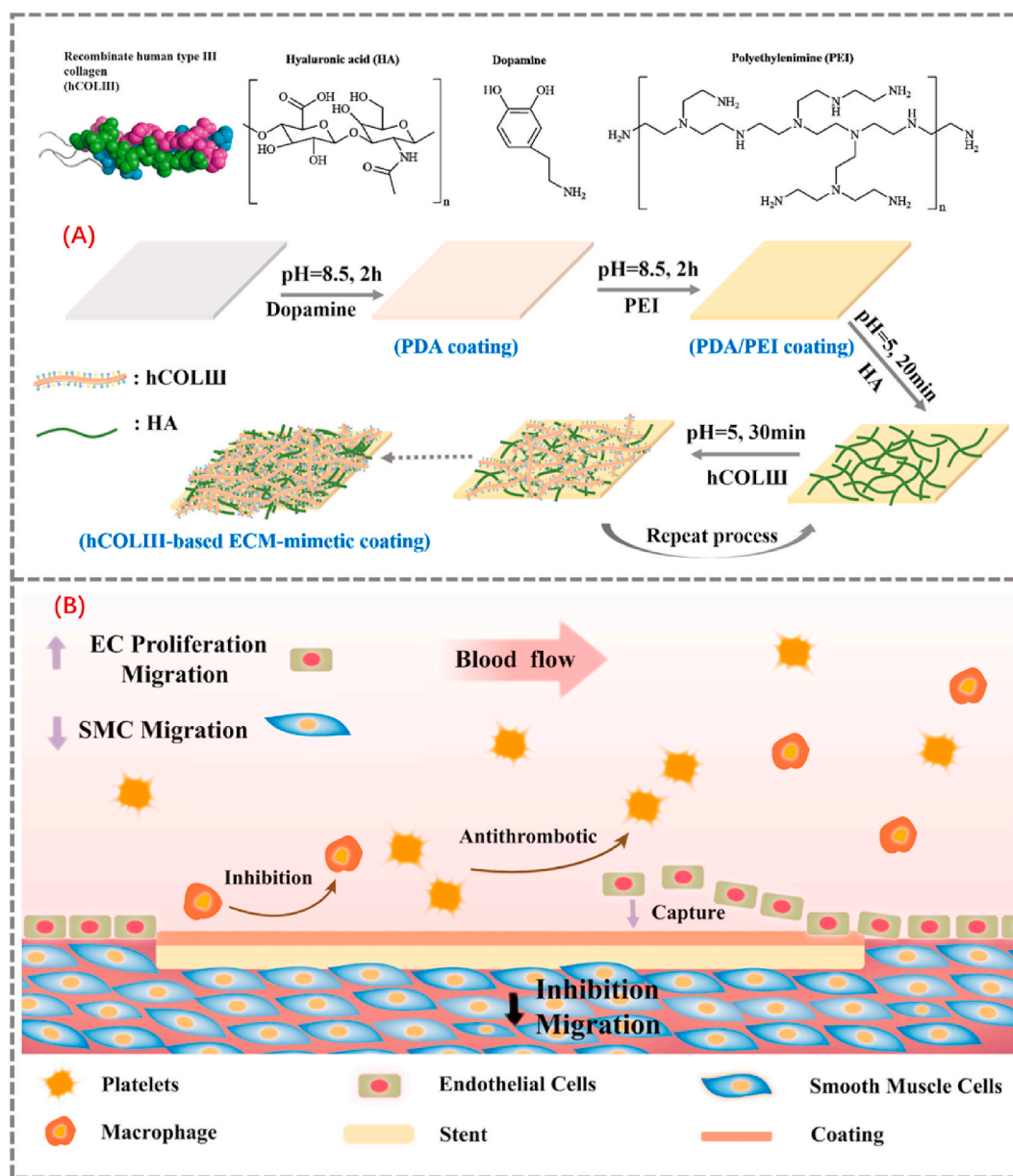
Scheme 1. Components of the ECM-mimetic coating: recombinant human type III collagen (hCOLIII), hyaluronic acid (HA), dopamine, and poly (ethylenimine) (PEI). (A) Immersion of the substrates in dopamine and PEI solution and subsequent alternative deposition of HA and hCOLIII to prepare an ECM-mimetic coating; and (B) the proposed mechanism of the ECM-mimetic coating with the function of anti-platelet adhesion, anti-inflammatory response and directing enhanced endothelialization and suppressed SMC proliferation.

Herein, a recombinant human type III collagen (hCOLIII) was developed that possesses a stable triple-helix conformation and contains multiple charged residues, including both Gly-Glu-Arg (GER) and Gly-Glu-Lys (GEK) triplets. Similarly, hCOLIII was derived from active peptide sequences in human type III collagen, while Gly483-Pro512 retained the highly adhesive fragments and circumvented the sequences containing hydroxyproline (O). The adhesion and activation of platelets on hCOLIII covered substrates was evaluated to ensure the lack of affinity of platelets for hCOLIII. Subsequently, an extracellular matrix mimetic (ECM-mimetic) coating was fabricated via stepwise deposition of hCOLIII and hyaluronic acid (HA) by layer-by-layer (LBL) assembly on an amine-rich polydopamine coated substrate (shown in Scheme 1). Compared with animal-derived collagen, the ECM-mimetic coating using the customized characteristics of hCOLIII was superior in suppressing the adhesion and activation of platelets. In vitro cell proliferation tests, including smooth muscle cells (SMCs) and endothelial cells (ECs), were used to evaluate the function of the coating in accelerating endothelialization and inducing the contractive phenotype of SMCs. Besides, the ECM-mimetic coating still showed the proprieties of enhancing anticoagulant and promoting endothelialization after exposure to phosphate buffer saline (PBS) for two weeks. With the ex vivo antithrombogenicity test, subcutaneous implantation, and in vivo stent implantation evaluation, the effects of the ECM-mimetic coating on mediating enhanced hemocompatibility, mild tissue response, promoted endothelialization and inhibition of excessive hyperplasia of neointima were demonstrated. This research highlights the potential of constructing collagen-based coatings for blood-contacting implants using a tailored recombinant human type III collagen.

2. Materials and methods

2.1. Materials and reagents

Silicon wafer (Si, 1×1 cm) was provided by Ningbo Sibranch International Trading Co., Ltd. Polylactic acid (PLA) sheets (1×1 cm) and vascular stents made of PLA were supplied by Sichuan Xingtai Pule Medical Technology Co., Ltd. For the QCM-D evaluation, AT-cut 5 MHz Au coated quartz crystal (10 mm in diameter) was obtained from Biolin Scientific (Sweden). The polyvinyl chloride (PVC) tube for the ex vivo thrombogenicity test was purchased from Tuyang Health Products Store. Dopamine hydrochloride (MW 189.64) and polyethyleneimine (MW 25000) was obtained from Sigma Aldrich. Hyaluronic acid (HA, MW 80 KDa-2000 KDa) was obtained from Aladdin (Shanghai). Reagents for hemocompatibility test, cell culture, and staining were mentioned in the corresponding section. Other reagents were local products of analytic grade.

2.2. Recombinant peptides derived from human type III collagen

All the related peptides derived from human type III collagen listed in Table 1 were synthesized by solid-phase peptide synthesis at Synpeptide Co., Ltd. (Nanjing, China). The peptides C3P1 and C3P2 without GER or GEK sequence or hydroxyproline (O) were principally considered as non-adhesive peptides, showing no affinity for cell or platelet adhesion. The peptides C3PO1 and C3PO2 were designed to contain GPO, and are expected to support platelet adhesion. T16WTp was the peptide containing the sequence of high cell adhesion affinity, derived from the Gly483-Pro512 sequence of the human type III collagen, while T16Op was the mutated design of T16WTp, which theoretically activated more platelets by introducing hydroxyproline (O). Overall, the recombinant human type III collagen (hCOLIII) reported here was demonstrated to be effective in significantly inhibiting the adhesion and activation of platelets, while it selectively supported the adhesion of cells, because of the existence of Gly483-Pro512 which contained adhesive segments like GER or GEK and obsoleted the sequence containing hydroxyproline (O). In addition, the localized charge distribution of the

Table 1
Amino acid sequences of the peptides derived from human type III collagen.

ID	Sequence	Purity	Notes
C3P1	Ac-GETGAPGLKGENGLPGENGAPGPMGPRGAP-NH$_2$	>95 %	1
C3P2	Ac-GQPGPPGPPGTAGFPGSPGAKGEVGPAGSP-NH$_2$	>95 %	1
C3PO1	Ac-GPAGPOGPOGPOGTSGHOGSOGSOGYQGPO-NH$_2$	>95 %	2
C3PO2	Ac-GPOGVAGPOGGSGPAGPOGPQGVKGERGSO-NH$_2$	>95 %	2
T16WTp	Ac-GERGAPGFRGPAGPNGIPGEKGPAGERGAP-NH$_2$	>95 %	3
T16Op	Ac-GERGAOGFRGPAGPNGIOGEKGPAGERGAO-NH$_2$	>95 %	4

Notes: (The letters are standard abbreviations of amino acids).
1- Expected to have low adhesion to cells or platelets.
2- Expected to induce platelets adhesion due to the introduction of hydroxyproline (O).
3- Expected to promote cell adhesion while do not support platelet adhesion.
4- Expected to support platelet adhesion due to the introduction of hydroxyproline (O).

adhesive segments might also affect the final performance.

2.3. Comparison of the binding affinity of platelets to diverse peptides

For validation of the above design concepts, it is essential to demonstrate the affinity of different peptides to platelets. In vitro platelet adhesion and activation were analyzed qualitatively on silicon wafers (Si) and polylactic acid (PLA) sheets. Detailed information is provided in Method S1 and Method S2 (Supplementary data). After further comparison, the T16WTp peptide was selected for synthesizing recombinant human type III collagen (hCOLIII). hCOLIII was composed of 16 tandem repeats of the triple-helix fragment of T16WTp. This protein was expressed in *Escherichia coli* (*E. coli*) and purified to be endotoxin-free under GMP condition (Shanxi Jinbo Biomedicine Co., Ltd., China).

2.4. Preparation of multilayered HA/collagen coating

Prior to the preparation of the multilayer coating, the substrates (Si or PLA) and PLA stents were pre-coated with a substrate-independent amine-rich polydopamine coating according to the scheme shown above. Briefly, the substrates were immersed in dopamine solution (2 mg/mL in tris buffer solution of pH 8.5) for 2 h and then immersed in polyethyleneimine solution (PEI, 20 mg/mL in tris buffer of pH 8.5) for another 2 h was prepared. The as-prepared coating was rich in amine groups, and named PDA/PEI. To fabricate the multilayer coating, the PDA/PEI treated samples were immersed in the HA solution (2 mg/mL, pH 5) for 20 min and rinsed with DI water 3 times (pH 5, each washing step 3 min). Then, the HA treated samples were transferred to a solution containing hCOLIII (2 mg/mL, pH 5) for further immersion for 20 min (three times rinsing with DI water). The above operation represented one cycle of the deposition with hCOLIII (positive charged polyelectrolytes) and HA (negative charged polyelectrolytes). The HA and hCOLIII were gradually deposited for several cycles, and the obtained samples were denoted as (HA/hCOLIII)x, where x referred to the number of the coating cycles. For comparison, multilayer coatings made of animal-derived collagen (aCOL) was used as a control, named (HA/aCOL)x, where x also indicates the number of the coating cycles. The stability of the (HA/hCOLIII)$_6$ coating on the stent surface was evaluated using FITC-labeled hCOLIII according to the same preparation protocol (Method S3).

2.5. Characterization

The surface elemental composition was evaluated by X-ray photoelectron spectroscopy (XPS) using Escalab 250Xi (Thermo Fisher

Scientific, USA) with an Al Ka achromatic X-ray source. The XPSPEAK41software was employed to fit the high-resolution XPS data.

Water contact angles were tested using Attension Theta (Biolin Scientific, Sweden). Surface zeta potential results were obtained with 0.1 mM KCl solution at pH 7.4 using SurPASS 3 (Anton Paar, Austria).

The morphologies of the samples were observed using atomic force microscopy (AFM) (Bruker Dimension Icon AFM, USA) and scanning electron microscopy (SEM) (FEI Quanta 450 FEG Environmental SEM).

2.6. Quartz crystal microbalance (QCM) evaluation

QCM was used as a powerful tool to investigate the in-situ growth of the polyelectrolyte multilayer coatings [27]. The frequency changes indicate adsorption and desorption at the material/liquid interface [28]. Herein, an AT-cut 5 MHz Au coated quartz crystal (10 mm in diameter) was used to study the stepwise deposition of hCOLIII and HA, using Q-sense analyzer (Biolin Scientific, Sweden). The crystals were pre-coated with PDA/PEI coating as described above and then assembled in the testing cell of the Q-sense analyzer. Then, DI water (pH 5) was pumped into the channel to adequately rinse the PDA/PEI coating to reach a stable baseline. After that, HA solution (2 mg/mL) and hCOLIII solution (2 mg/mL) were pumped into the channel at a rate of 50 μL/min to perform several cycles of the alternate deposition steps. The frequency-time curve was recorded to monitor the growth behaviors of the multilayer coatings.

2.7. Biocompatibility evaluation

2.7.1. Platelets adhesion test

In vitro platelet adhesion was determined to study the binding affinity of platelets on (HA/hCOLIII)x coatings, including lactate dehydrogenase (LDH, Beyotime Biotechnology) and morphological observation of the adhered platelets. Blood from New Zealand White Rabbits with citrate as the anticoagulant [29] was centrifugated at 1500 r/min for 15 min, and the supernatant was carefully collected as platelet-rich plasma (PRP). After that, the samples were incubated with PRP for 60 min at 37 °C, followed by washing with PBS and fixation with 2.5 % glutaraldehyde solution for at least 12 h. Then the platelet morphologies on the surfaces were observed by SEM. The LDH assay was performed according to the protocol described in Method S2.

2.7.2. Ex-vivo thrombogenicity evaluation

The ex vivo thrombogenicity test was carried out using an arteriovenous shunt model at New Zealand white rabbits (2.5–3 kg) [30]. The PLA tube and (HA/hCOLIII)n coated tubes (n = 3, 6, 12, and 15) were installed and connected with an extracorporeal bypass from the carotid artery to the jugular vein. The experiment was stopped after 2 h of circulation, then the blood clots harvested from the samples and the cross-section of the tubes were further analyzed to study the thrombogenicity of different samples. The detailed information of the ex vivo study is shown in Method S4.

2.7.3. ECs proliferation

Primary human umbilical vein endothelial cells (HUVECs) at the second passage were cultured in RPMI 1640 media containing 10 % (v/v) fetal bovine serum (FBS) and 1 % (v/v) penicillin-streptomycin at 37 °C in an atmosphere with 5 % carbon dioxide [31]. The samples were immersed in 75 % alcohol for 3 h for sterilization and cultured with 1 mL ECs suspension (2.5×10^4 cells/mL) for 1 and 3 days with medium change every 24 h. The cell morphology was evaluated by Fluorescein diacetate (FDA, 167 μg/mL, dissolved in acetone in the dark)/Propidium iodide (PI, 10 μg/mL) staining for 3 min. After that, the FDA and PI solution were removed, and the samples were gently washed with PBS. A fluorescence microscope (Nikon, TE2000) was used to observe the morphologies of cells. The cell viability at 1 day and 3 days was measured by CCK-8 assay (fresh RPMI 1640 medium containing CCK-8

(9:1, v/v)), and the absorbance value at 450 nm was read [32].

2.7.4. SMCs proliferation and determination of phenotype

Human umbilical artery smooth muscle cells (HUASMCs) were cultured with HyClone™ DMEM (GE Life Sciences, China), containing 1 % penicillin-streptomycin and 10 % fetal bovine serum (FBS); other processes and methods were similar to those mentioned above in the HUAECs compatibility test. To determine the phenotype of SMCs, Western Blot (WB) was conducted to analyze the expression of phenotypic markers of SMCs, including contractile phenotype markers, such as α-smooth muscle actin (α-SMA), transgelin or Smooth muscle 22a (SM22a), and the synthetic phenotype markers, including matrix metalloproteinases-2, and -9 (MMP-2, MMP-9), following the protocol in Method S5 [33].

2.7.5. Subcutaneous implantation test

The animal experiments were done in accordance with the ethical standards and animal use regulations of the China Council on Animal Care and the Sichuan University animal use protocol (approval No. KS2020394). The PLA, HA/aCOL, and HA/hCOLIII multilayer-coated PLA sheets were implanted into the subcutaneous tissue of adult SD rats. The methods of implantation and staining are described in Method S6, and the implanting scheme is shown in Figure S1 (Supplementary data).

2.7.6. Stent implantation evaluation

Bare PLA stents, rapamycin-eluting PLA stents (provided by Sichuan Xingtai Pule Medical Technology Co., Ltd, drug loading 8 μg/mm), and HA/hCOLIII coated PLA stents were implanted in the abdominal aorta of rabbits. Before the experiment, the stents were crimped on the balloon and sterilized, and then the balloon was expanded in the abdominal aorta of the rabbits. After 1 and 3 months of implantation, the vessels containing the stents were excised and rinsed with a heparin solution to avoid ongoing clot deposition on the surfaces of the inner vascular tissues. Then, the vessels embedded with stents were fixed by tissue fixation solution for one week for further evaluation, including H&E staining and immunohistochemical staining (by anti- CD68, -CD31, -eNOS, and -αSMA antibodies). In addition, the area of the vascular lumen and the endothelialization ratio were calculated by Image-J software. Imagepro-plus software was employed to assess the expression of eNOS and α-SMA [34]. The inflammation score was measured by CD68 staining according to the previous study [35]. The detailed process of the immunohistochemistry analysis is described in Method S7.

2.8. Statistical analysis

The data were expressed as mean value ± standard deviation (SD). All the data were analyzed using the software SPSS 11.5, performing one-way ANOVA to determine the statistical significance (*$p < 0.05$, **$p < 0.01$, and ***$p < 0.001$).

3. Results and discussion

3.1. Tailored recombinant human type III collagen

Antithrombotic equipment is always a challenge for blood-contacting devices, like vascular grafts, stents, artificial heart valves, and catheters [15,16]. For instance, the implantation of a stent damages the blood vessel wall and exposures the ECM matrix, mainly consisting of collagen, subsequently leading to thrombus formation. The thrombogenic feature of collagen is mainly ascribed to the binding affinity with platelets. The I domain of the platelet receptor $α_2β_1$ recognizes and binds collagen through the sequences GFOGER, GLOGER, GROGER, GLOGEN, etc., which promotes the design of the recombinant collagen fragments without the hydroxyproline (O) containing sequences. The peptides derived and synthesized from human type III collagen were

investigated here. As illustrated in Table 1, two categories of peptides derived from human type III collagen were selected, namely C3P1/C3P2 and T16WTp, which were expected to represent the non-adhesive and adhesive peptides, respectively.

Compared with the PLA substrate, the amount and activation degree of the adherent platelets on the C3P1 and C3P2 coated samples were obviously reduced, as seen in Fig. 1, indicating that the peptides without hydroxyproline (O) sequence were not prone to support platelet adhesion. Interestingly, T16WTp that possessed the highly active sequences GER and GEK, which demonstrated to promote vessel cell adhesion before [20,21], did not induce severe platelet adhesion and activation. However, after introducing hydroxyproline (O), the adhesion and activation of platelet by the peptides C3PO1, C3PO2, and T16Op were dramatically enhanced. The number of platelets adhering to the samples is shown in Figure S2, where T16Op caused the most severe adhesion/activation of platelets. A similar phenomenon was found in the tests using Si wafers as the substrates (Figure S3). These data strongly suggested that the targeted sequence of peptides without hydroxyproline (O) effectively eluded the binding to platelets, while T16WTp is a tailored peptide derived from human type III collagen, which synergistically promotes the adhesion of endothelial cells without binding platelets.

The recombinant human type III collagen (hCOLIII, 45 kDa, Figure S5) was synthesized after the tandem repeat design of T16WTp, with good water solubility, compared with animal-derived collagen (Figure S6). The adhesion and activation of platelets were further evaluated by comparison with animal-derived collagen. As shown in Fig. 1, almost no platelet adhered on both substrates after covering with hCOLIII. In contrast, the animal-derived collagen (aCOL) supported numerous platelets to adhere, and these platelets were severely activated. The quantification of the adherent platelets (Figure S4) also demonstrated the efficiency of hCOLIII in repressing platelet adhesion, suggesting that hCOLIII might be a tailored collagen-derived material to prepare surface coatings for blood-contacting devices.

3.2. Stepwise assembly of HA/hCOLIII coating

The high water solubility of hCOLIII made the current coatings on the substrates, obtained via direct immersion, not stable enough for long-term use in a physiological environment. Therefore, layer-by-layer (LBL) assembly was adopted to prepare a fully extracellular matrix (ECM) mimetic coating by the stepwise deposition of HA and hCOLIII (Scheme 1).

QCM-D is a versatile and applicable means for monitoring the formation process of LBL multilayer coatings. The frequency change has a negative correlation with the mass adsorbed on the surface [28]. Fig. 2A shows the stepwise assembly process of HA and hCOLIII in several initial cycles. The LBL assembly included the following steps: (1) UP water rinsing to reach a stable baseline; (2) the adsorption of negatively charged HA, followed with DI water rinsing; (3) the adsorption of positively charged hCOLIII, followed with DI water rinsing; (4) rinsing using PBS after several repeated cycles to evaluate the stability of the assembled components.

The recombinant hCOLIII consisted of 16 tandem repeats of the triple-helix fragments of human type III collagen, Gly483-Pro512 (Figure S5). The repeated GER and GEK sequences provided abundant arginine (R) and lysine (K) that are alkaline amino acids, which endowed the hCOLIII with a positively charged surface. Therefore, the alternative deposition of the negatively-charged HA and the positively-charged hCOLIII became possible. Continuous deposition of both HA and hCOLIII is shown in Fig. 2A, which followed the classical electrostatic force-induced LBL assembly [36,37]. The strength of attraction
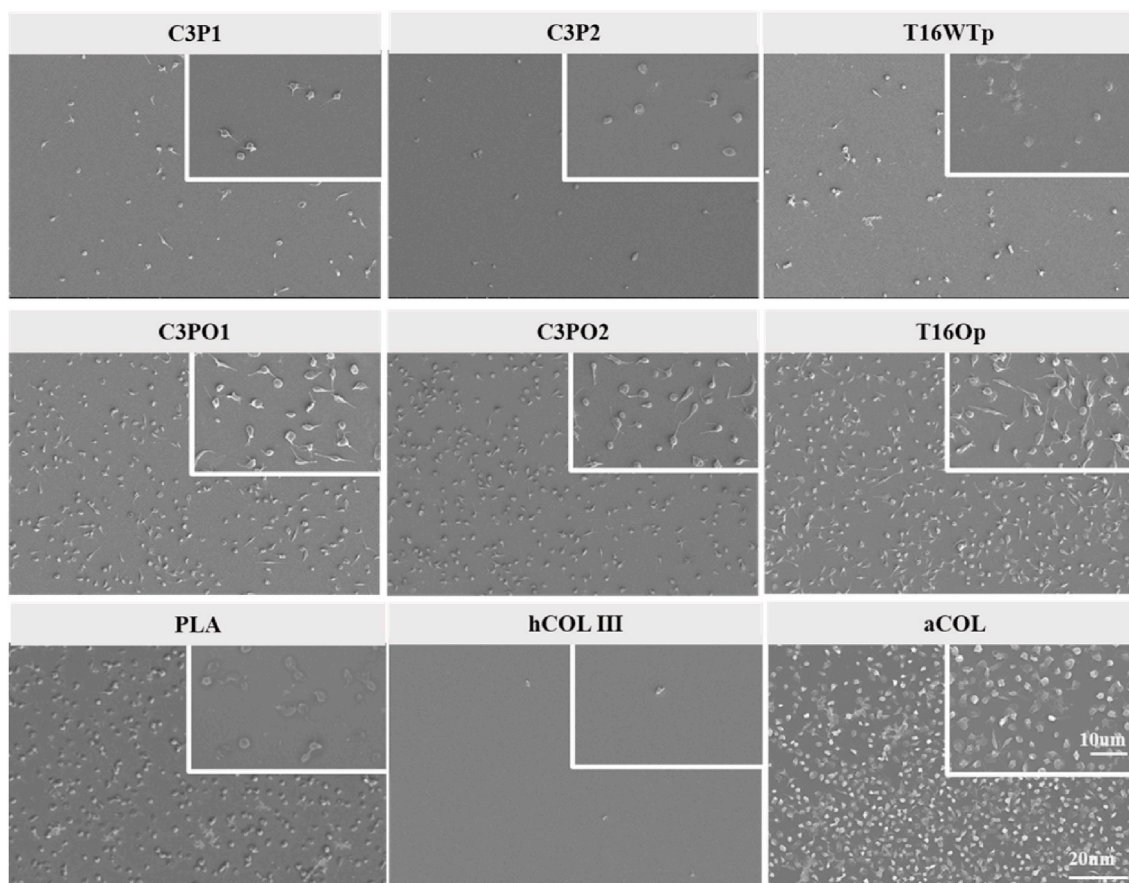

Fig. 1. SEM images of adherent platelets on different peptides/proteins covered PLA substrates.
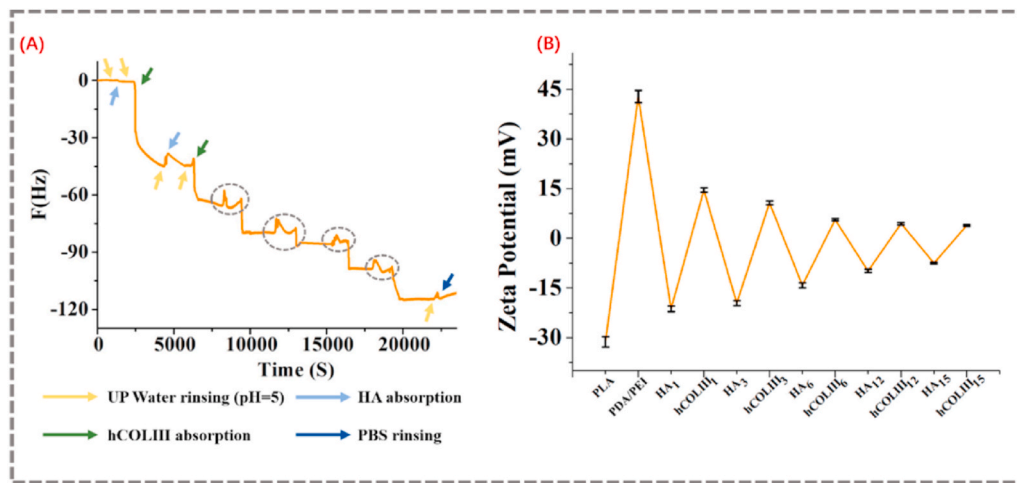
Fig. 2. (A) QCM-D monitoring of the stepwise deposition process of HA and hCOLIII; (B) the zeta potential data of the alternative outmost layer by HA and hCOLIII at different cycles collected under pH 7.4.

and stability of the coating in a physiological environment needs careful evaluation [38]. The frequency change was about 116 Hz after the deposition of 6 cycles, and only 5 Hz of decrease was found during rinsing in PBS at the last stage, indicating that the multilayer coating had adequate stability against PBS rinsing. Noticeably, more layers of deposition would form a coating mixed with more HA and collagen. The outmost layer is not pure collagen or HA, but a composite surface.

The surface zeta potential around pH 7.4 is shown in Fig. 2B. The zeta potential of the PLA substrate was about -30 mV at pH 7.4, while the zeta potential of the PDA/PEI surface was about $+37$ mV indicating the presence of amine-rich groups. The alternating change on the surface zeta potential presented after the stepwise introduction of HA and hCOLIII. The range of shift in the zeta potential became smaller and smaller with the increase of the coating cycles, indicating that the surface charge was more balanced, where the zeta potential of (HA/hCOLIII)$_{12}$ and (HA/hCOLIII)$_{15}$ were around 0 mV. This phenomenon also showed good agreement with previous reports using LBL assembly to

prepare multilayer coatings, with the increase of LBL layer numbers, the alternative deposition of positive and negative charge polyelectrolytes would prepare a surface being electrically neutral [37,38]. In general, the QCM-D and zeta potential results verified the successful stepwise assembly of the (HA/hCOLIII)x coating.

3.3. Characterization

The surface morphology and roughness of the coatings were evaluated using AFM. Usually, stepwise deposition of macromolecules on substrates has a gradually increased surface roughness. As shown in Fig. 3A, the root mean square (RMS) roughness of PLA substrate was about 0.82 nm, which gradually increased by increasing the number of cycles, reaching 88.11 nm on the (HA/hCOLIII)$_{15}$ coating.

The elemental information of each layer in the (HA/hCOLIII)x coatings was analyzed by XPS. Fig. 3B presents the wide scan spectra of the different samples, and Figure S7 presents the elemental ratio of the
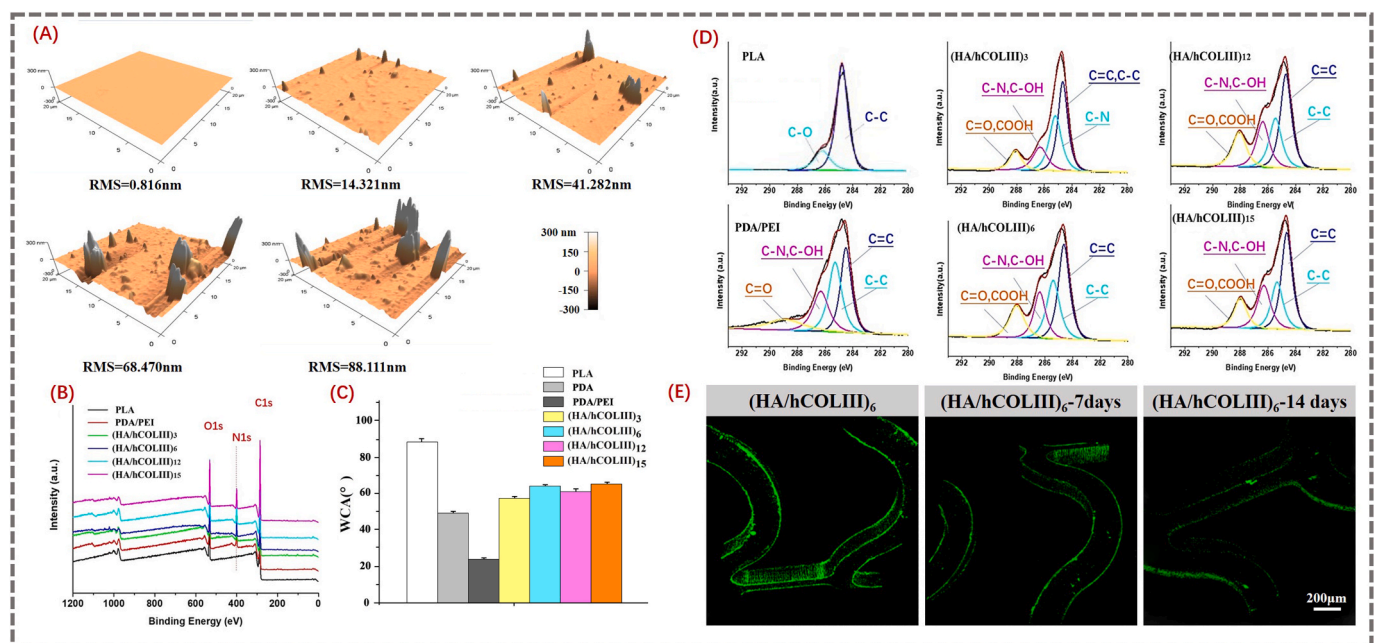

Fig. 3. (A) The surface morphology and roughness of substates covered with different coating cycles; (B) XPS wide scan spectrum of the surface elements; (C) water contact angle of different samples; (D) the high resolution of C1s spectrum of different cycles of the HA/hCOLIII coatings; (E) fluorescence signal on (HA/hCOLIII)$_6$ after 7 and 14 days of immersion in PBS.

outmost layer with hCOLIII at different cycles. Compared with the bare PLA substrate, the occurrence of the nitrogen signal directly proved the successful pre-treatment with the PDA/PEI coating. There were only the signals of the C, N and O elements in the (HA/hCOLIII)x coatings (x = 3, 6, 12, 15) with the deposition of HA and collagen. The surface became more hydrophilic after (HA/hCOLIII)x coating (Fig. 3C). The C1s high-resolution spectra of the samples also conformed to the following binding forms in Fig. 3D: 288.3 eV (CO–NH, quinone C=O, COO-), 286.5 eV (C–N, C–OH and phenol hydroxyl), 285.0 eV (C–C, C–H), and 284.5 eV (C=C). The C=C bonds were ascribed to the introduction of PDA/PEI, containing catechol rings [39]. The peaks corresponding to C–OH and COOH indicated that the deposited HA and hCOLIII increased with increasing coating cycles, and reached a relatively steady state after 6 cycles. This demonstrated that surface composition with the outmost layer of hCOLIII reached a stable condition, as the information obtained through XPS was for the film-depth of around 10 nm [40].

The water contact angle (WCA) results further supported the conclusions. The abundance of amino groups increased the hydrophilicity of the samples after coating with PDA/PEI to a WCA of about 25°. The coating became less hydrophilic after the deposition of the HA/hCOLIII coatings, with the WCA ranging from 50° to 70° (Fig. 3C).

Once implanted, the coating would respond to the blood microenvironment at the initial stage of implantation. Vascular cells (endothelial cells, smooth muscle cells, and even macrophages) would adhere to the coating surface and gradually cover them to form a neointima, usually after one- or two-week implantation. Therefore, during this stage, the coating with recombinant human type III collagen should maintain the ability of enhancing anticoagulant and promoting endothelialization. The QCM-D data indicated that the coating had sufficient stability when immersed in PBS at the initial stage (Fig. 2A). The retention of hCOLIII on the coating was evaluated by fluorescent labeling. Fig. 3E presents the fluorescence signals on a PLA stent covered by (HA/hCOLIII)$_6$ coating using FITC-labeled hCOLIII. There was no major attenuation of the fluorescence after one week of immersion, which confirmed the adequate stability of the (HA/hCOLIII)$_6$ coating in PBS in one week. There were also fluorescence signals even after two-week immersion, implying that the coating was stable to perform the properties after implantation. The above results confirmed that more deposited layers could induce higher coverage ratio of hCOLIII and HA, endowing the composite coating with reliable and longer anti-coagulant ability. After immersion in PBS solution for two weeks, it could still present significant anti-platelet adhesion ability, compared with PLA substrates.

3.4. Hemocompatibility test

Hemocompatibility is a basic requirement of blood-contacting devices. Device implantation is usually associated with the adhesion and denaturation of serum proteins, the adhesion and activation of platelets, and combined interactions, ultimately leading to thrombus formation [41]. The tailored feature of hCOLIII in suppressing platelet adhesion
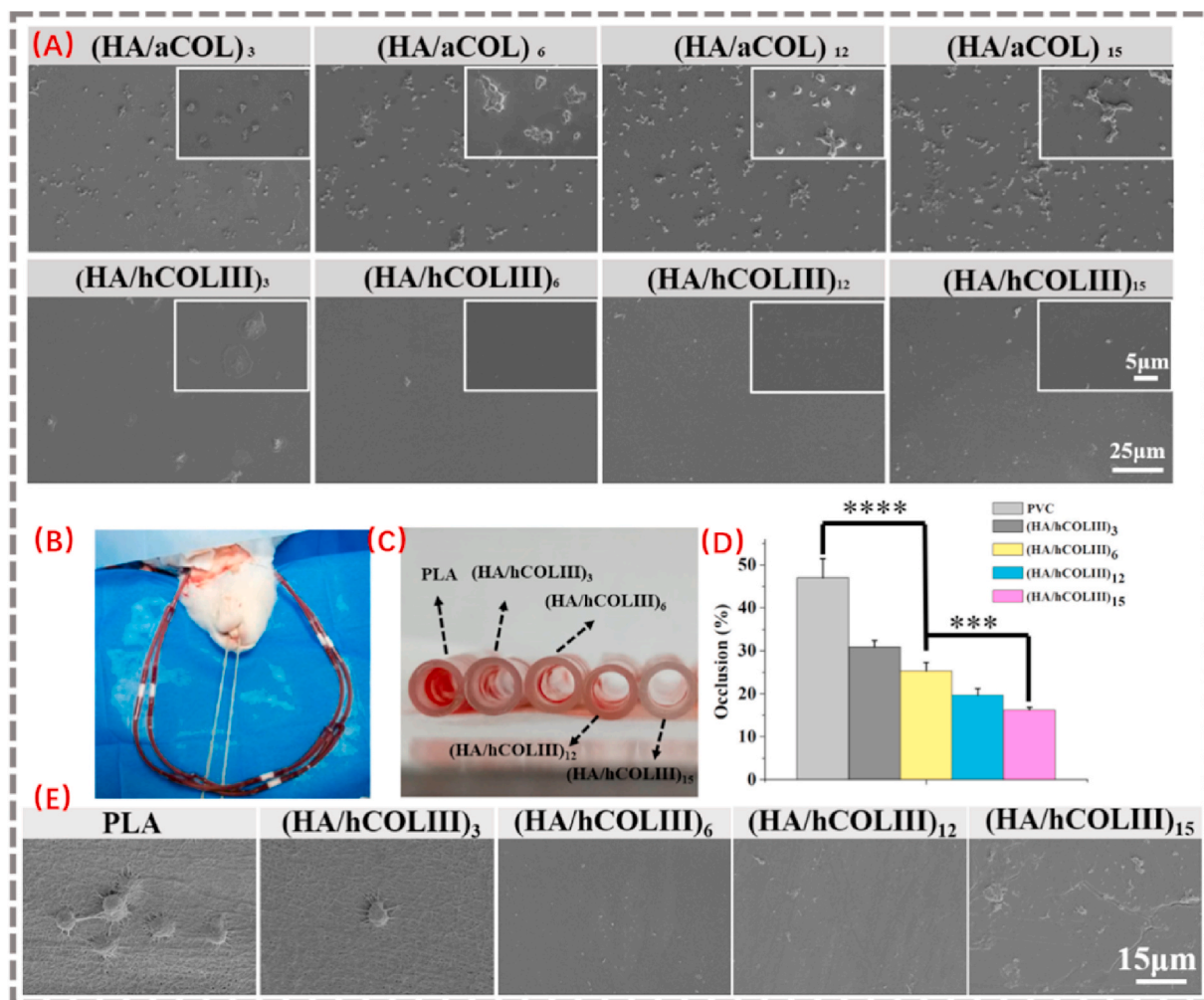

Fig. 4. (A) Platelets adhesion/activation on multilayer coatings with different cycles prepared using HA and aCOL or hCOLIII, respectively; (B) photo of the arteriovenous extracorporeal circuit; (C) photo of the deposited thrombus and (D) occlusion rate on different tubes; (E) SEM images of the deposited components on the different surfaces after circulation for 2 h.

was demonstrated in Fig. 1. The surfaces covered by the negatively charged HA also attracted moderate platelet adhesion/activation in Figure S8.

The platelet adhesion/activation after incubation on the different samples is shown in Fig. 4A. The (HA/aCOL)x coatings (x = 3, 6, 12, 15)

prepared with animal-derived collagen caused severe platelet adhesion/activation. By contrast, the (HA/hCOLIII)x (x = 3, 6, 12, 15) coating effectively suppressed the adhesion of platelets. It is noteworthy that, although (HA/hCOLIII)₃ coating also had fewer platelet adhesion, some platelets were activated, which may be ascribed to incomplete coverage
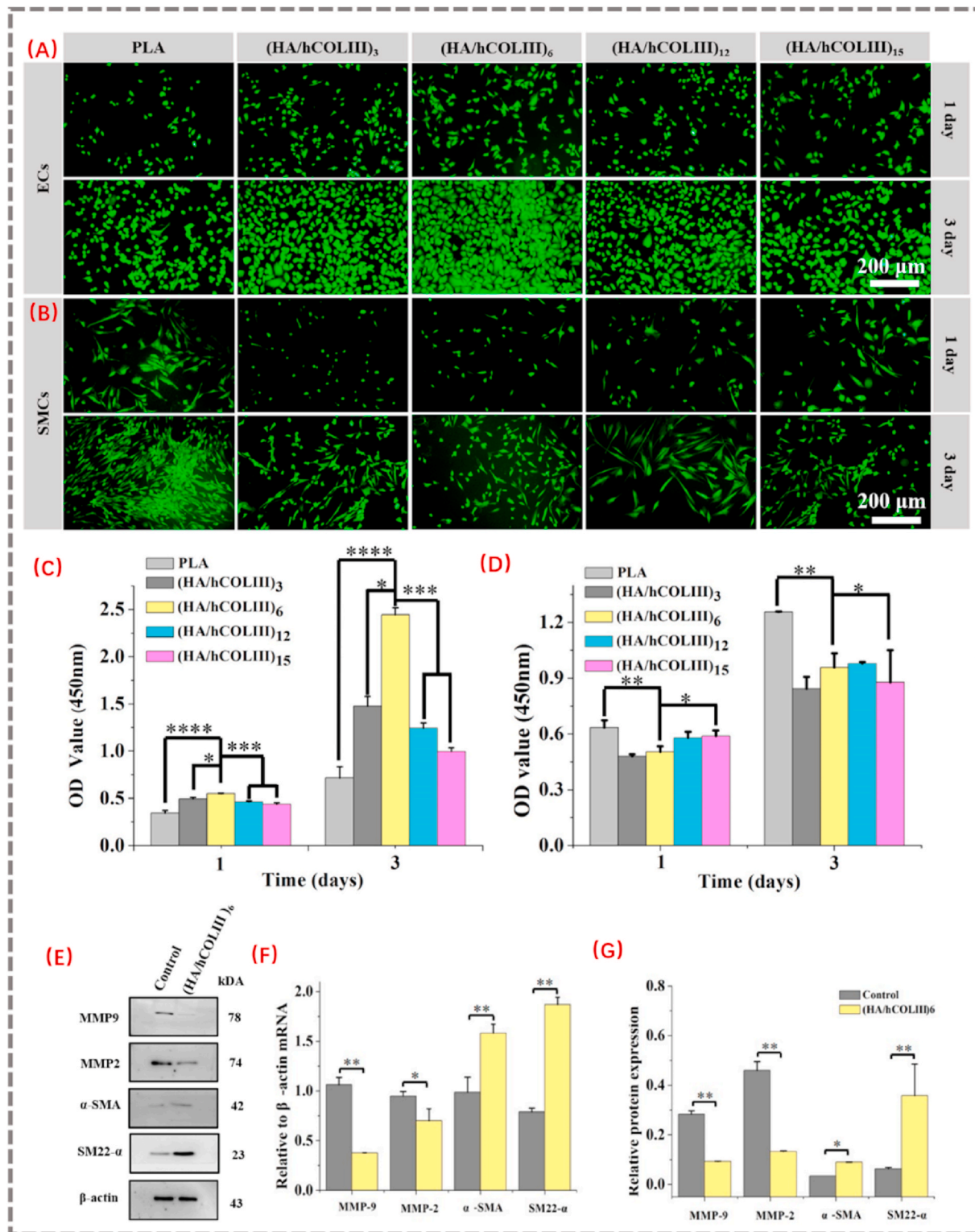

Fig. 5. (A) Fluorescent staining of (A) ECs and (B) SMCs after 1 day and 3 days culture on different samples; The cell viability result of (C) the ECs and (D) SMCs on different samples; (E) Western Blotting analysis of the expression of cytoskeletal proteins, including smooth muscle 22a (SM22a), α-smooth muscle actin (α-SMA), and extracellular matrix-related components, including matrix metalloproteinases-2, -9 (MMP-2, MMP-9); (F) Quantification of the expression of cytoskeletal proteins; (G) the mRNA expression of α-SMA, SM22a, MMP-2, and MMP-9.

of the HA/hCOLIII components.

The coatings immersed in PBS for two weeks were also employed to evaluate the anti-adhesive property of (HA/hCOLIII)x (x = 3, 6, 12, 15) coatings, and they also performed well in suppressing platelet adhesion in vitro, as shown in Figure S9, which once more confirms the sufficient stability of the coatings.

The thrombotic behavior of the different samples was studied in the ex vivo circulation model (Fig. 4B). As shown in Fig. 4C, the PLA tube resulted in severe thrombus deposition during 2-h circulation, and (HA/hCOLIII)$_3$ coating also induced thrombus deposition. However, more coating cycles of HA/hCOLIII highly inhibited the thrombus deposition and resulted in a lower occlusion rate (Fig. 4D). SEM images of the inner side of the tubes are shown in Fig. 4E, indicating that the online ex vivo thrombotic evaluation was in good agreement with the in vitro platelets adhesion results and further proved the antithrombotic performance of the HA/hCOLIII coatings. Different from aCOL, hCOLIII did show its potential as a tailored collagen coating for blood-contacting materials.

3.5. In vitro cell proliferation and phenotype switching of SMCs

Enhanced endothelialization is essential after stent implantation. Thus, developing a functional surface coating that can effectively promote the healing of the endothelium layer is a hot research topic [42]. Our previous work demonstrated that the recombinant human type III collagen promotes cell adhesion [20]. Endothelial cell proliferation induced by hCOLIII was also confirmed in this study (Figure S10). The effect of the (HA/hCOLIII) coatings on the proliferation of ECs and SMCs were also investigated. Compared with PLA substrate, all the (HA/hCOLIII)x (x = 3, 6, 12, 15) coatings effectively enhanced the proliferation of ECs in Fig. 5A and B, and only quite few dead ECs (red fluorescence) appeared on the (HA/COLIII)X coatings after 1 and 3 days culturing, respectively (Figure S11A). The results showed that the ECM-mimetic coatings containing hyaluronic acid and recombinant collagen accelerated the endothelialization process. The (HA/hCOLIII)$_6$ coating showed the best ECs viability, while (HA/hCOLIII)$_{12}$ and (HA/hCOLIII)$_{15}$ coatings presented reduced support of ECs proliferation, probably due to the surface charge, as both (HA/hCOLIII)$_{12}$ and (HA/hCOLIII)$_{15}$ coating had a zeta potential near +0 mV (Fig. 2B). The coating there behaved like a zwitterion surface, which might diminish the ability to support cell adhesion at the initial stage of contact, and eventually led to a slight decrease in the proliferation of ECs.

Suppressing the proliferation of SMCs is a desired property to restrain the neointima hyperplasia after stent implantation [43]. As commonly accepted, during the stages of human atherosclerotic plaque development, SMCs are the dominant cells. During the formation of atherosclerotic plaques, the phenotype switching of SMCs from contractile to synthetic is also typical during the SMC accumulation in the neointima [44].

As seen in Figure S12, the recombinant human type III collagen also supported the enhanced proliferation of SMCs. However, once hCOLIII formed the multilayer (HA/hCOLIII)x coating, suppressed proliferation of SMCs was observed, compared with PLA (Fig. 5C and D). The number of living SMCs on (HA/COLIII)x coatings also showed an evident decline than PLA after 1 and 3 days culturing, respectively (Figure S11B)." There was no obvious red signal on the (HA/COLIII)x, indicating that the coating could suppress the proliferation of SMCs by mediating their phenotype instead of killing them. Western Blotting (WB) was conducted to analyze the expression of phenotypic markers of SMCs and elucidate the underlying mechanism. The contractile phenotype markers, such as smooth muscle 22a (SM22a), α-smooth muscle actin (α-SMA), showed up-regulated expression in SMCs in the presence of (HA/hCOLIII)$_6$, whereas the synthetic phenotype markers matrix metalloproteinases 2 and 9 (MMP-2, MMP-9), were significantly decreased (Fig. 5E and F). Consistently, the α-SMA and SM22a mRNA expression of MMP-2 and MMP-9 showed lower levels in HA/hCOLIII (Fig. 5G). These results indicated that the (HA/hCOLIII)$_6$ inhibited the synthetic

phenotype of SMCs, associated with aberrant proliferation, and the SMCs presented a more contractile phenotype that might indicate suppressed proliferation. This result was consistent with the result of Live/Dead assay of SMCs. While the mechanism behind it is not fully understood and is still under investigation.

The different receptors between ECs and SMCs might also direct the diverse behaviors, as hCOLIII interacted with the cells via integrins. The multilayer coating with HA might also contribute to the promotion of the contractile phenotype of SMCs [45]. In total, the data demonstrated the potential of HA/hCOLIII coating as a tailored collagen-based material with good hemocompatibility, supporting ECs proliferation and suppressing SMCs proliferation.

To refine the subsequent animal studies, (HA/hCOLIII)$_6$ coating was prepared on PLA sheets and PLA stents to evaluate the tissue response and in situ endothelialization further.

3.6. In vivo inflammatory response

The inflammatory response around the material/tissue interface has an essential impact on the outcome of an implantation. Macrophages adhere to the biomaterial surface after implantation, and quickly produce inflammatory cytokines, reaching a peak concentration within 24 h [46]. Moreover, the materials influence local tissue response and direct fibrous encapsulation [47]. Higher degrees of inflammatory cell infiltration cause stronger development of granulation tissue and thicker fibrous coating, as signs of more serious tissue reaction [35].

Fig. 6A shows the HE stains of the tissues harvested after subcutaneous implantation for 15 and 30 days. Fig. 6B presents the CD68 stains, reflecting the inflammatory cell infiltration. Thicker encapsulation occurred for PLA (26.0 ± 2.0 μm) and (HA/aCOL)$_6$ (28.9 ± 4.6 μm) after the implantation for 15 days. On the contrary, the thickness of the capsule around (HA/hCOLIII)$_6$ sample was much lower (15.8 ± 2.5 μm) in Fig. 6C. According to the results of CD68 staining, more inflammatory cells infiltrated the newly formed capsules on the PLA and (HA/aCOL)$_6$ samples, while there were quite a few inflammatory cells in the capsules on (HA/hCOLIII)$_6$ samples (Fig. 6D). A similar phenomenon was also found on the capsules formed after 30 days of implantation. The reason why the cellularity of the (HA/hCOLIII)$_6$ group decreasing between 15 and 30 days was that a fibrous capsule tissue gradually matured and the inflammatory response became attenuated on (HA/hCOLIII)$_6$ with the extension of time. Compared with the PLA and animal-derived collagen-based coatings, the recombinant human type III collagen-based (HA/hCOLIII)$_6$ coating supported low inflammatory response and good tissue compatibility.

3.7. In vivo endothelialization and neointima formation

The rabbit abdominal aorta model was implanted in vivo to evaluate the feasibility of the (HA/hCOLIII)$_6$ coating in promoting in situ endothelialization and inhibiting excessive intimal hyperplasia. In addition to a bare PLA stent, a rapamycin-eluting stent (RAPA) was implanted and used as a control. The (HA/hCOLIII)x coatings were prepared on the inner and outer lumen of the stent. After implantation for 1 month, the vessels with stent struts were harvested and stained by HE, anti-CD68, and *anti*-αSMA to investigate the restenosis rate, inflammation response, and maturity of the neointima. As seen in Figure S12, the restenosis rate of bare PLA stent was about 37.2 ± 2.5 %, much lower than for the RAPA stent (14.6 ± 2.7 %) and (HA/hCOLIII)$_6$ stent (15.2 ± 3.1 %). Besides, due to the release of rapamycin, which also has anti-inflammatory activity [48], the inflammatory response was sharply decreased compared with the PLA stent. However, on the (HA/hCOLIII)$_6$ stent, the inflammation score was even lower without a specific anti-inflammatory drug. As described above, the endothelial cell layer in the intima would be damaged and then SMCs would be exposed during stent implantation, so the coating on the outer side of the stent would contact with SMCs and ultimately the (HA/hCOLIII)$_6$ coating would
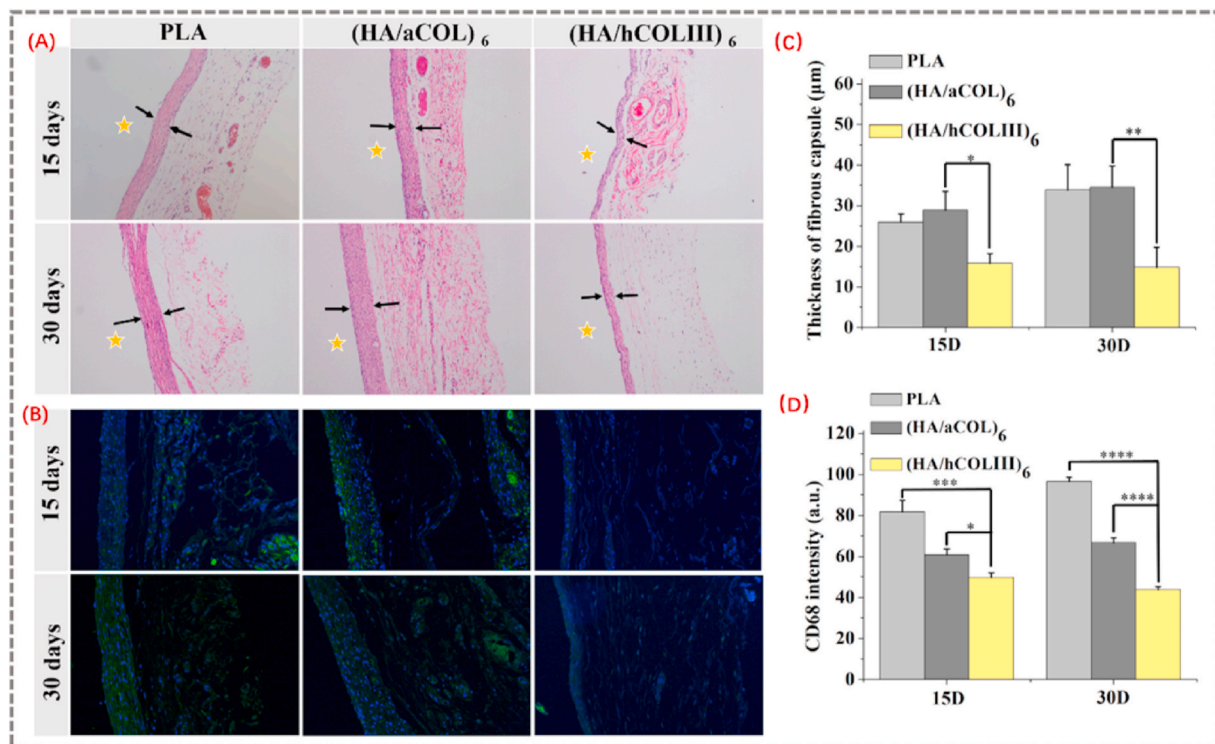
Fig. 6. (A) HE staining of the tissues harvested after subcutaneous implantation for 15 and 30 days; (B) CD68 staining of the tissues; (C) thickness of the fibrous capsules of different samples; (D) relative immunofluorescence intensity of CD68 of the capsules of different samples. Asterisks were labeled the location of implantation samples.

induce a more contractile phenotype of SMCs. Thus, the αSMA intensity on the SMCs around (HA/hCOLIII)$_6$ stent was also highest, indicating that SMCs were more in a contractile phenotype, which was also a hint of the more mature neointima.

Inhibition of SMCs phenotypic switching was associated with a reduced accumulation of macrophages, suggesting that the inflammatory cytokines from SMCs largely contributed to the accumulation of macrophages [49]. Therefore, the global gene expression profile of SMCs cultured on the (HA/hCOLIII)x was analyzed. As seen in Figure S13, the biological process (BP) analysis indicated that the (HA/hCOLIII)$_6$ coating regulated the inflammatory biological processes in SMCs. KEGG analysis revealed the potential signal pathways regulating the inflammatory response in SMCs. The differently expressed genes related to inflammation in SMCs cultured on (HA/hCOLIII) also presented. Furthermore, proinflammation factors (TNF-α, IL-6 and IL-1β) were suppressed in SMCs cultured on the (HA/hCOLIII)$_6$ coating on both gene and protein levels.

The stents embedded in the blood vessel tissues were harvested after implantation for 3 months. The restenosis rate, inflammation score, and α-SMA intensity are presented in Fig. 7A–D. They showed a similar tendency with the data obtained from stents implanted for 1 month. The suppressed proliferation of SMCs and the inhibited inflammatory response on (HA/hCOLIII)$_6$ stent synergistically led to the low restenosis rate. During stent implantation, the endothelial cell layer in the intima would be damaged and then SMCs would be exposed, so the coating on the outer side of the stent would contact with SMCs and ultimately regulate their function.

The endothelialization potential was further evaluated by the investigation of the enface neointima. There were different morphologies in Fig. 7E, which indicated different cell types/conditions on the neointima. The cells covered on the PLA and RAPA stent surface were in an irregular state, consisting of different cells or secreted extracellular matrix, indicating immature endothelialization. The cells on the neointima of the (HA/hCOLIII)$_6$ stent presented a paving stone shape, which

is the typical endothelial cell style [50]. A detailed CD31, eNOS, and DAPI immunofluorescence staining was performed to evaluate the enfaced endothelium state (Fig. 7F–I). According to the DAPI staining, the cell density on the (HA/hCOLIII)$_6$ stent surface (3079 cells/mm^2) was significantly higher than on the PLA (2483 cells/mm^2) and RAPA (2356 cells/mm^2) stent surface after three months in Fig. 7F. For a better comparison, the CD68 and αSMA expression rates of the abdominal aorta of New Zealand rabbits was set as 100 % (Figure S14). It was found that the CD31 expression of the cells on the PLA stent struts and RAPA stent struts was about 52.9 % and 62.9 %, respectively. The rapamycin-eluting stent strongly inhibits the formation of the neointima, and the released drug also causes an immature healing of the endothelium layer. The eNOS expression as a key function of endothelial cells reflects the total endothelialization degree on different stents [51]. Compared with the (HA/hCOLIII)$_6$ stent, the eNOS signal was much lower on the PLA (37.6 %) and RAPA (44.6 %) stent. These results suggested that the coating provided a beneficial microenvironment for promoting the in situ endothelialization and realizing the function of endothelial cells. The comparison with the RAPA stent indicated the potential of the ECM-mimetic coating in realizing desired neointima growth in vivo. Normally healthy animal models are directly used to perform the anticoagulation and anti-proliferation properties study to evaluate the safety of the stents [1,3]. We also realize that animal models with corresponding diseases are critical to the studies related to atherosclerotic disease research, therefore, the design of the atherosclerosis model to verify the function of the coating would be considered in the future studies.

4. Conclusion

In this work, a recombinant human type III collagen (hCOLIII) was synthesized, in which the adhesive sequence contains GER and GEK, without hydroxyproline (O). Unlike animal-sourced collagen, the specially prepared hCOLIII effectively eliminated the binding site with
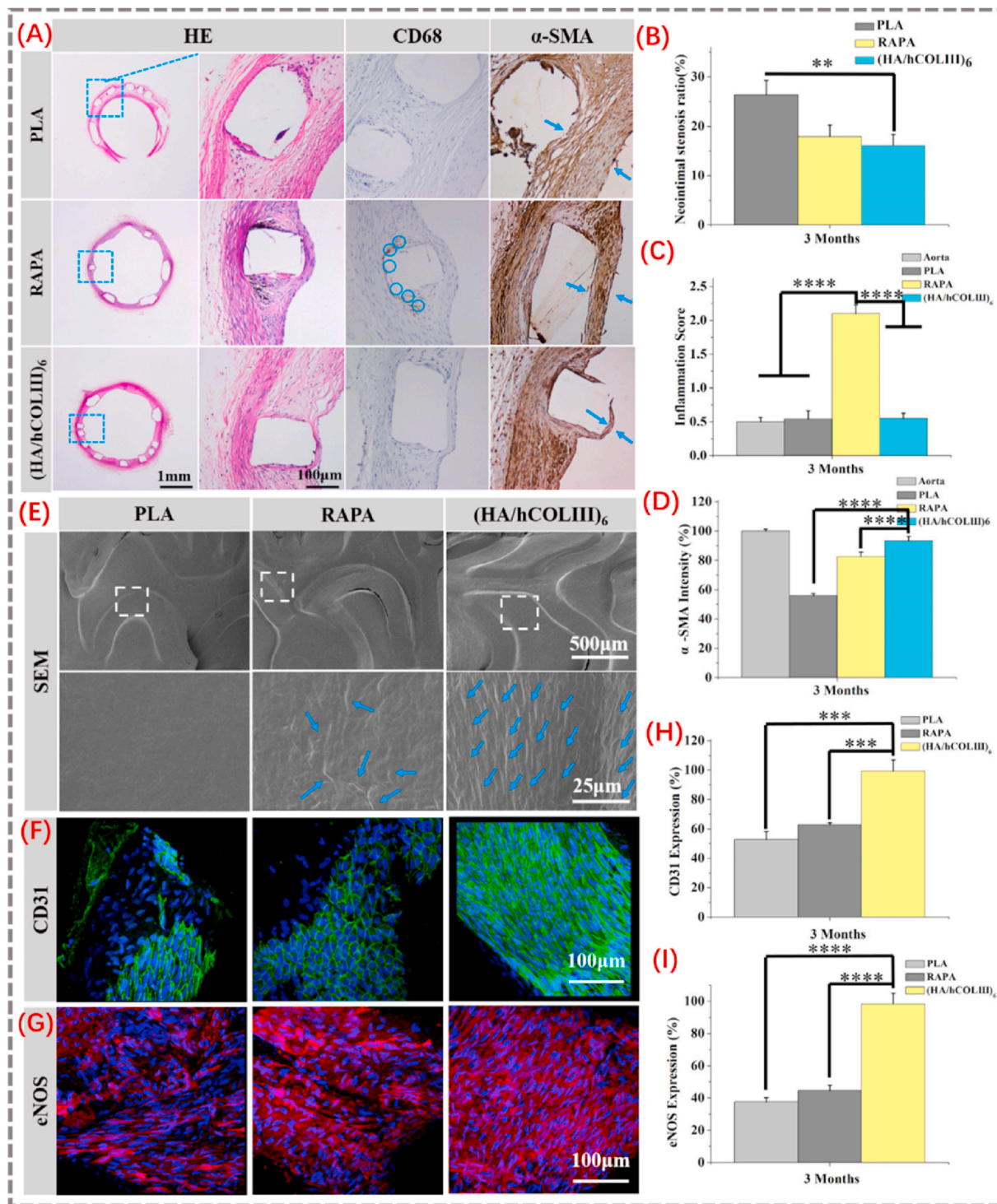
Fig. 7. (A) Immunohistochemical staining of the circular tissues around implanted stents by staining of HE, CD68, and α-SMA; (B) the stenosis rate of the vessels; (C) and the inflammation score of different tissues; (D) and the relative intensity of α-SMA in the tissues; (E) SEM view of the inner side of the tissues; (F) the CD31 expression and (G) eNOS expression on the enface of the neointima; and (H, I) the quantitative intensity of expressed CD31 and eNOS on the enface of the neointima.

platelets, providing a prospect for blood-contacting applications. An ECM-mimetic coating was prepared by the stepwise assembly of HA and hCOLIII. The platelet adhesion/activation and ex vivo antithrombotic tests confirmed excellent hemocompatibility for the ECM-mimetic coating. The hCOLIII-based ECM-mimetic coating not only presented mild inflammatory response of the tissue but also showed ideal guiding of the cell fate by promoting the proliferation of ECs and inhibiting the proliferation of SMCs via promoting the contractile phenotype. In vivo

stent implantation data demonstrated the function of the ECM-mimetic coating in promoting in situ endothelialization and suppressing the excessive neointima hyperplasia, which provided a novel approach for developing functional coatings of cardiovascular stents using collagen-based materials.

Declaration of competing interest

The authors declare that they have no known competing financial interests or personal relationships that could have appeared to influence the work reported in this paper.

Acknowledgements

Appendix A. Supplementary data

Supplementary data to this article can be found online at https://doi.org/10.1016/j.biomaterials.2021.121055.

Credit author statement

Li Yang, Methodology, Conceptualization, Data curation, Formal analysis, Writing – original draft. Haoshuang Wu, Validation, Formal analysis, Visualization, Software. Lu Lu, Formal analysis, Resources. Qing He, Writing, Software Boting Xi, Resources. Hongchi Yu, Formal analysis. Rifang Luo, Resources, Formal analysis, Writing – review & editing, Supervision, Funding acquisition. Yunbing Wang, Resources, Formal analysis, Writing – review & editing, Supervision, Funding acquisition. Xingdong Zhang, Resources, Formal analysis.

Data availability statement

The raw/processed data required to reproduce these findings cannot be shared at this time as the data also forms part of an ongoing study. Anyone who are interested in this study can contact the corresponding authors to obtain more information.

References

[1] I. Cockerill, C.W. See, M.L. Young, Y. Wang, D. Zhu, Designing better cardiovascular stent materials: a learning curve, Adv. Funct. Mater. 31 (2021) 2005361, https://doi.org/10.1002/adfm.202005361.

[2] N. Lyu, Z. Du, H. Qiu, P. Gao, Z. Yang, Mimicking the nitric oxide-releasing and glycocalyx functions of endothelium on vascular stent surfaces, Adv. Sci. 7 (2020) 2002330, https://doi.org/10.1002/advs.202002330.

[3] J.B. Slee, I.S. Alferiev, C. Nagaswami, J.W. Weisel, S.J. Stachelek, Enhanced biocompatibility of CD47-functionalized vascular stents, Biomaterials 87 (2016) 82–92, https://doi.org/10.1016/j.biomaterials.2016.02.008.

[4] Bai, J. Zhao, M. Wang, Y. Feng, J. Ding, Matrix-metalloproteinase-responsive gene delivery surface for enhanced in situ endothelialization, ACS Appl. Mater. Interfaces 12 (2020) 40121–40132. https://pubs.acs.org/doi/10.1021/acsami.0c11971.

[5] M.F. Maitz, M.C.L. Martins, N. Grabow, C. Matschegewski, N. Huang, E.L. Chaikof, M.A. Barbosa, C. Werner, C. Sperling, The blood compatibility challenge Part 4: surface modification for hemocompatible materials: passive and active approaches to guide blood-material interactions, Acta Biomater. 94 (2019) 33–43, https://doi.org/10.1016/j.actbio.2019.06.019.

[6] H. Qiu, Q. Tu, P. Gao, X. Li, Z. Yang, Phenolic-amine chemistry mediated synergistic modification with polyphenols and thrombin inhibitor for combating the thrombosis and inflammation of cardiovascular stents, Biomaterials 269 (2021) 120626, https://doi.org/10.1016/j.biomaterials.2020.120626.

[7] J. Yang, Y. Zeng, C. Zhang, Y.-X. Chen, Z. Yang, Y. Li, X. Leng, D. Kong, X.-Q. Wei, H.-F. Sun, C.-X. Song, The prevention of restenosis in vivo with a VEGF gene and paclitaxel co-eluting stent, Biomaterials 34 (2013) 1635–1643, https://doi.org/10.1016/j.biomaterials.2012.11.006.

[8] Y. Liu, A. Mahara, Y. Kambe, Y.-I. Hsu, T. Yamaoka, Endothelial cell adhesion and blood response to hemocompatible peptide 1 (HCP-1), REDV, and RGD peptide sequences with free N-terminal amino groups immobilized on a biomedical expanded polytetrafluorethylene surface, Biomaterials Science (2021), https://doi.org/10.1039/D0BM01396J.

[9] X. Luo, C. Han, P. Yang, A. Zhao, N. Huang, The co-deposition coating of collagen IV and laminin on hyaluronic acid pattern for better biocompatibility on cardiovascular biomaterials, Colloids Surf. B Biointerfaces 196 (2020) 111307, https://doi.org/10.1016/j.colsurfb.2020.111307.

[10] J.L. Chen, Q.L. Li, J.Y. Chen, C. Chen, N. Huang, Improving blood-compatibility of titanium by coating collagen–heparin multilayers, Appl. Surf. Sci. 255 (2009) 6894–6900, https://doi.org/10.1016/j.apsusc.2009.03.011Get rights and content.

[11] K.S. Silvipriya, K.K. Kumar, A.R. Bhat, B.D. Kumar, A. John, P. Lakshmanan, Collagen: animal sources and biomedical application, J. Appl. Pharmaceut. Sci. 5 (2015) 123–127, https://doi.org/10.7324/JAPS.2015.50322.

[12] X. Wu, W. Li, K. Chen, D. Zhang, X. Yang, A tough PVA/HA/COL composite hydrogel with simple process and excellent mechanical properties, Materials Today Communications 21 (2019) 100702, https://doi.org/10.1016/j.mtcomm.2019.100702.

[13] H.R.B. Raghavendran, S. Mohan, K. Genasan, M.R. Murali, S.V. Naveen, T. Kamarul, Synergistic interaction of platelet derived growth factor (PDGF) with the surface of PLLA/Col/HA and PLLA/HA scaffolds produces rapid osteogenic differentiation, Colloids Surf. B Biointerfaces 139 (2016) 68–78, https://doi.org/10.1016/j.colsurfb.2015.11.053.

[14] D. Naskar, P. Bhattacharjee, A.K. Ghosh, M. Mandal, S.C. Kundu, Carbon nanofiber reinforced nonmulberry silk protein fibroin nanobiocomposite for tissue engineering applications, ACS Appl. Mater. Interfaces 9 (2017) 19356–19370, https://doi.org/10.1021/acsami.6b04777.

[15] F. Zhang, C. Hu, L. Yang, K. Liu, Y. Ge, Y. Wei, J. Wang, R. Luo, Y. Wang, A conformally adapted all-in-one hydrogel coating: towards robust hemocompatibility and bactericidal activity, J. Mater. Chem. B 9 (2021) 2697–2708, https://doi.org/10.1039/D1TB00021G.

[16] Y. Wang, B. Ma, K. Liu, R. Luo, Y. Wang, A multi-in-one strategy with glucose-triggered long-term antithrombogenicity and sequentially enhanced endothelialization for biological valve leaflets, Biomaterials 275 (2021) 120981, https://doi.org/10.1016/j.biomaterials.2021.120981.

[17] H.Y. Chow, Y. Zhang, E. Matheson, X. Li, Ligation technologies for the synthesis of cyclic peptides, Chem. Rev. 119 (2019) 9971–10001, https://doi.org/10.1021/acs.chemrev.8b00657.

[18] Y. Zhou, Z. Lu, X. Wang, J.N. Selvaraj, G. Zhang, Genetic engineering modification and fermentation optimization for extracellular production of recombinant proteins using Escherichia coli, Appl. Microbiol. Biotechnol. 102 (2018) 1545–1556, https://doi.org/10.1016/j.biortech.2014.09.035.

[19] P.G. Manfredini, V.A.F. Cavanhi, J.A.V. Costa, L.M. Colla, Bioactive peptides and proteases: characteristics, applications and the simultaneous production in solid-state fermentation, Biocatal. Biotransform. (2020) 1–19, https://doi.org/10.1080/10242422.2020.1849151.

[20] C. Hua, Y. Zhu, W. Xu, S. Ye, R. Zhang, L. Lu, S. Jiang, Characterization by high-resolution crystal structure analysis of a triple-helix region of human collagen type III with potent cell adhesion activity, Biochem. Biophys. Res. Commun. 508 (2019) 1018–1023, https://doi.org/10.1016/j.bbrc.2018.12.018.

[21] S. You, S. Liu, X. Dong, H. Li, Y. Zhu, L. Hu, Intravaginal administration of human type III collagen-derived biomaterial with high cell-adhesion activity to treat vaginal atrophy in rats, ACS Biomater. Sci. Eng. 6 (2020) 1977–1988, https://doi.org/10.1021/acsbiomaterials.9b01649.

[22] W.R. Surin, M.K. Barthwal, M. Dikshit, Platelet collagen receptors, signaling and antagonism: emerging approaches for the prevention of intravascular thrombosis, Thromb. Res. 122 (2008) 786–803, https://doi.org/10.1016/j.thromres.2007.10.005.

[23] B.P. Nuyttens, T. Thijs, H. Deckmyn, K. Broos, Platelet adhesion to collagen, Thromb. Res. 127 (2011) S26–S29, https://doi.org/10.1016/S0049-3848(10)70151-1.

[24] C.G. Knight, L.F. Morton, A.R. Peachey, D.S. Tuckwell, R.W. Farndale, M.J. Barnes, The Collagen-binding A-domains of Integrins α1β1 and α2β1recognize the same specific amino acid sequence, GFOGER, in native (Triple-helical) collagens, J. Biol. Chem. 275 (2000) 35–40, https://doi.org/10.1074/jbc.275.1.35.

[25] T. Wang, J. Lew, J. Premkumar, C.L. Poh, M.W. Naing, Production of recombinant collagen: state of the art and challenges, Engineering Biology 1 (2017) 18–23, https://doi.org/10.1049/enb.2017.0003.

[26] M.M. Schmidt, R.C.P. Dornelles, R.O. Mello, E.H. Kubota, M.A. Mazutti, A.P. Kempka, I.M. Demiate, Collagen extraction process, International Food Research Journal 23 (2016) 913–922.

[27] N.J. Cho, C.W. Frank, B. Kasemo, F. Höök, Quartz crystal microbalance with dissipation monitoring of supported lipid bilayers on various substrates, Nat. Protoc. 5 (2010) 1096–1106, https://doi.org/10.1038/nprot.2010.65.

[28] L. Yang, L. Li, H. Wu, B. Zhang, R. Luo, Y. Wang, Catechol-mediated and copper-incorporated multilayer coating: an endothelium-mimetic approach for blood-contacting devices, J. Contr. Release 321 (2020) 59–70, https://doi.org/10.1016/j.jconrel.2020.02.002.

[29] F. Yang, L. Xu, D. Kuang, Y. Ge, G. Guo, Y. Wang, Polyzwitterion-crosslinked hybrid tissue with antithrombogenicity, endothelialization, anticalcification properties, Chem. Eng. J. 24 (2020) 128244, https://doi.org/10.1016/j.cej.2020.128244.

[30] B. Zhang, R. Yao, L. Li, Y. Wang, Y. Wang, Green tea polyphenol induced Mg2+-rich multilayer conversion coating: toward enhanced corrosion resistance and promoted in situ endothelialization of AZ31 for potential cardiovascular applications, ACS Appl. Mater. Interfaces 11 (2019) 41165–41177, https://doi.org/10.1021/acsami.9b17221.

[31] J. Lu, W. Zhuang, L. Li, B. Zhang, Y. Wang, Micelle-embedded layer-by-layer coating with catechol and phenylboronic acid for tunable drug loading, sustained release, mild tissue response, and selective cell fate for Re-endothelialization, ACS

Appl. Mater. Interfaces 11 (2019) 10337–10350, https://doi.org/10.1021/acsami.9b01253.

[32] Y. Chen, S. Zhao, B. Liu, M. Chen, G. Wan, Corrosion-controlling and osteo-compatible Mg ion-integrated phytic acid (Mg-pa) coating on magnesium substrate for biodegradable implants application, ACS Appl. Mater. Interfaces 6 (2014) 19531–19543, https://doi.org/10.1021/am506741d.

[33] S. Allahverdian, C. Chaabane, K. Boukais, G.A. Francis, M.L. Bochaton-Piallat, Smooth muscle cell fate and plasticity in atherosclerosis, Cardiovasc. Res. 114 (2018) 540–550, https://doi.org/10.1093/cvr/cvy022.

[34] K.-S. Park, S.N. Kang, D.H. Kim, H.-B. Kim, K.S. Im, W. Park, Y.J. Hong, D.K. Han, Y.K. Joung, Late endothelial progenitor cell-capture stents with CD146 antibody and nanostructure reduce in-stent restenosis and thrombosis, Acta Biomater. 111 (2020) 91–101, https://doi.org/10.1016/j.actbio.2020.05.011.

[35] R.S. Schwartz, E. Edelman, R. Virmani, A. Carter, J.F. Granada, G.L. Kaluza, N.A. F. Chronos, K.A. Robinson, R. Waksman, J. Weinberger, Drug-eluting stents in preclinical studies updated consensus recommendations for preclinical evaluation, Circulation Cardiovascular Interventions 1 (2) (2008) 143, https://doi.org/10.1161/CIRCINTERVENTIONS.108.789974.

[36] Y.M. Zhao, L.H. Li, B. Li, C.R. Zhou, LBL coating of type I collagen and hyaluronic acid on aminolyzed PLLA to enhance the cell-material interaction, Express Polym. Lett. 8 (2014) 322–335, https://doi.org/10.3144/expresspolymlett.2014.36.

[37] J. Zhang, B. Senger, D. Vautier, C. Picart, P. Lavalle, Natural polyelectrolyte films based on layer-by layer deposition of collagen and hyaluronic acid, Biomaterials 26 (2005) 3353–3361, https://doi.org/10.1016/j.biomaterials.2004.08.019.

[38] M. Tang, X. Zhu, Y. Zhang, Z. Zhang, Z. Zhang, Q. Mei, J. Zhang, M. Wu, J. Liu, Y. Zhang, Near-infrared excited orthogonal emissive upconversion nanoparticles for imaging-guided on-demand therapy, ACS Nano 13 (9) (2019) 10405–10418, https://doi.org/10.1021/acsnano.9b04200.

[39] K.H. Bae, K. Lee, C. Kim, T.G. Park, Surface functionalized hollow manganese oxide nanoparticles for cancer targeted siRNA delivery and magnetic resonance imaging, Biomaterials 32 (2011) 176–184, https://doi.org/10.1016/j.biomaterials.2010.09.039.

[40] C. Das, M. Wussler, T. Hellmann, T. Mayer, W. Jaegermann, In situ XPS study of the surface chemistry of MAPI solar cells under operating conditions in vacuum, Phys. Chem. Chem. Phys. 20 (2018) 17180–17187, https://doi.org/10.1039/C8CP01259H.

[41] J. Wang, Y. Chen, Y. Chen, J. Li, Fabrication and characterization of superhydrophilic and antibacterial surfaces by silver nanoparticle self-assembly,

Colloid Polym. Sci. 295 (2017) 2191–2196, https://doi.org/10.1007/s00396-017-4179-5.

[42] Q. Zhao, J. Wang, Y. Wang, H. Cui, X. Du, A stage-specific cell-manipulation platform for inducing endothelialization on demand, National Science Review 7 (2019) 629–643, https://doi.org/10.1093/nsr/nwz188.

[43] Q. Gao, X. Li, W. Yu, F. Jia, T. Yao, Q. Jin, J. Ji, Fabrication of mixed-charge polypeptide coating for enhanced hemocompatibility and anti-infective effect, ACS Appl. Mater. Interfaces 12 (2020) 2999–3010, https://doi.org/10.1021/acsami.9b19335.

[44] G. Douglas, E. Van Kampen, A.B. Hale, E. McNeill, J. Patel, M.J. Crabtree, Z. Ali, R. A. Hoerr, N.J. Alp, K.M. Channon, Endothelial cell repopulation after stenting determines in-stent neointima formation: effects of bare-metal vs. drug-eluting stents and genetic endothelial cell modification, Eur. Heart J. 34 (2012) 3378–3388, https://doi.org/10.1093/eurheartj/ehs240.

[45] K. Qin, F. Wang, R.M. Simpson, X. Zheng, H. Wang, Y. Hu, Q. Zhao, Hyaluronan promotes the regeneration of vascular smooth muscle with potent contractile function in rapidly biodegradable vascular grafts, Biomaterials 257 (2020) 120226, https://doi.org/10.1016/j.biomaterials.2020.120226.

[46] T.N. Tulenko, M. Chen, P.E. Mason, R.P. Mason, Physical effects of cholesterol on arterial smooth muscle membranes: evidence of immiscible cholesterol domains and alterations in bilayer width during atherogenesis, JLR (J. Lipid Res.) 39 (1998) 947, https://doi.org/10.1089/jir.1998.18.351.

[47] F. Otsuka, A.V. Finn, S.K. Yazdani, M. Nakano, F.D. Kolodgie, R. Virmani, The importance of the endothelium in atherothrombosis and coronary stenting, Nat. Rev. Cardiol. (2012) 439–453, https://doi.org/10.1038/nrcardio.2012.64.

[48] A.D. Luna-Preitschopf, H. Zwickl, S. Nehrer, M. Hengstschläger, M. Mikula, Rapamycin maintains the chondrocytic phenotype and interferes with inflammatory cytokine induced processes, Int. J. Mol. Sci. 18 (2017) 1494, https://doi.org/10.3390/ijms18071494.

[49] S. Allahverdian, P.S. Pannu, G.A. Francis, Contribution of monocyte-derived macrophages and smooth muscle cells to arterial foam cell formation, Cardiovasc. Res. 95 (2012) 165–172, https://doi.org/10.1093/cvr/cvs094.

[50] Y. Liu, J. Lu, H. Li, J. Wei, X. Li, Engineering blood vessels through micropatterned co-culture of vascular endothelial and smooth muscle cells on bilayered electrospun fibrous mats with pDNA inoculation, Acta Biomater. 11 (2015) 114–125, https://doi.org/10.1016/j.actbio.2014.10.004.

[51] R.J. Smith, B. Nasiri, J. Kann, D. Yergeau, J.E. Bard, D.D. Swartz, S.T. Andreadis, Endothelialization of arterial vascular grafts by circulating monocytes, Nat. Commun. 11 (2020) 1–16, https://doi.org/10.1038/s41467-020-15361-2.